Carrier lifetime measurement of perovskite films by differential microwave photoconductivity decay

Keisuke Ohdaira[1], Huynh Thi Cam Tu[1], Ai Shimazaki[2], Ryuji Kaneko[2], Yuka Sumai[3], Md. Shahiduzzaman[3], Tetsuya Taima[3], and Atsushi Wakamiya[2]

[1]Japan Advanced Institute of Science and Technology, Nomi, Ishikawa 923-1292, Japan

[2]Institute for Chemical Research, Kyoto University, Uji, Kyoto 611-0011, Japan

[3]Nanomaterials Research Institute, Kanazawa University, Kakuma, Kanazawa, Ishikawa 920-1192, Japan

We measure the minority carrier lifetime of perovskite films by differential microwave photoconductivity decay (μ-PCD). Clear decay curves can be detected from bare and laminated methylammonium lead iodide ($MAPbI_3$) films by the differential μ-PCD. The degradation of the bare and laminated $MAPbI_3$ films under air exposure at room temperature is clearly observed as the continuous change of the decay curves. The differential μ-PCD can thus be a quick and non-destructive method for the characterization of the electrical quality of perovskite films and modules.

In recent years, new-type thin-film solar cells with an absorber consisting of perovskite crystal, so-called perovskite solar cells, have attracted much attention because of their superior conversion efficiency.[1–17] The photovoltaic (PV) application of the perovskite films is not limited to single-layered cells but also to tandem cells with conventional materials. In particular, perovskite/silicon (Si) tandem solar cells have been expected as next-generation high-efficiency cells since the fabrication process of crystalline Si solar cells has been highly matured and the current PV market share has been dominated almost completely by Si wafer-based solar cells.[18–23] In the perovskite/Si tandem solar cells, their module structures must be similar to those of conventional crystalline Si PV modules since a perovskite top cell will be formed on a Si wafer-based bottom cell. The lamination process for the conventional crystalline Si PV modules is performed typically at 100–150 °C, at which some of perovskite materials, such as methylammonium lead iodide ($MAPbI_3$), can be thermally degraded.[24–26] The degradation of the perovskite films during and after the lamination process should thus be readily evaluated for the selection of encapsulant materials and for the optimization of lamination conditions.

Microwave photoconductivity decay (μ-PCD) has been widely used as a conventional, non-contact, and non-destructive method for the evaluation of the minority carrier lifetime of Si wafers.[27–31] A pulse light irradiation generates excess carriers in an absorber, which enhances the reflection of microwave. The recombination of the excess carriers results in the decrease of microwave reflection, and a carrier lifetime can be evaluated from the decay of the microwave reflection. μ-PCD is applicable not only for bare Si wafers but for laminated Si wafers and cells.[30,31] Furthermore, μ-PCD can be used also for the characterization of thin films by using a high-sensitivity system—differential μ-

PCD.[28,29] In the differential μ-PCD, microwave reflections are measured at two neighboring positions with and without excess carrier excitation, resulting in higher sensitivity by taking the difference of microwave reflection intensity at the two positions. This technique is expected to be utilized for the evaluation of perovskite films; however, to the best of our knowledge, there has been little work for the μ-PCD measurement of perovskite films, although similar technique has been already proposed.[32,33] This might be due to the existence of already well-known time-resolved photoluminescence (TRPL). The demonstration of evaluating laminated perovskite films by differential μ-PCD will also lead to the future evaluation of laminated perovskite single cells and perovskite/Si tandem cells. In this note, we report the results on the differential μ-PCD measurement for $MAPbI_3$ films for the carrier lifetime measurement. The minority carrier lifetimes of both bare and laminated films are evaluated by differential μ-PCD.

We prepared 400-nm-thick $MAPbI_3$ films directly on glass substrates with a size of 26×28×0.7 (t) mm. $MAPbI_3$ solution was first synthesized by dissolving 1 M PbI_2 and 1 M CH_3NH_3I (MAI) in DMF:DMSO (4:1) mixed solvent and stirring at 70 °C for 60 min, and was then spin-coated on the glass substrates using antisolvent technique with chlorobenzene, followed by heating on a hotplate at 100 °C for 60 min.[16,17] Some $MAPbI_3$ films were then laminated by using a module laminator (NPC, LM-50X50-S) to form small-sized glass-glass modules consisting of 3.2-mm-thick cover glass/thermoplastic polyolefin elastomer (TPO) encapsulant/$MAPbI_3$ sample/TPO encapsulant/cover glass. The TPO encapsulant was highly transparent in an ultraviolet wavelength region. The lamination was divided into two processes: degassing process by evacuation at 110 °C for 30 min and adhesion process at a pressure of 60 kPa at 110 °C for 10 min. The bare and laminated $MAPbI_3$ films were stored in air at room temperature

in the dark.

The $MAPbI_3$ films before and after air exposure were characterized by differential μ-PCD (KOBELCO, LTA-1510EP). A $LiYF_4$ third harmonic generation pulse laser with a wavelength of 349 nm and a pulse duration of ~30 ns was used for the generation of excess carriers in $MAPbI_3$ films. An areal photon density of a laser pulse is $\sim 2\times10^{14}$ /cm^2. Note that this corresponds to an excess carrier density (Δn) of $\sim 5\times10^{18}$ /cm^3 if all the photons are absorbed in $MAPbI_3$ and excited carriers are distributed uniformly in a 400-nm-thick $MAPbI_3$ film. This assumption is reasonable since the diffusion coefficient of carriers in $MAPbI_3$ is 1.35 cm^2/s[34] and resulting diffusion length is >400 nm for a duration of >1 ns. Microwave with a frequency of 26 GHz was used for the measurement. The phase of the 26 GHz microwave was tuned so that the intensity of the reflected microwave was maximized. The tuning of the microwave phase will also contribute to the cancellation of the influence of bottom silicon when the perovskite/Si tandem structures are evaluated in the future.

Figure 1 shows a decay curve obtained by differential μ-PCD from an as-prepared bare $MAPbI_3$ film. One can see a first sharp increase in the microwave reflection intensity, indicating the irradiation of pulse light and resulting formation of excess carriers. The intensity of the microwave reflection then decreases with time by carrier recombination. The slope of the decay curve, which generally corresponds to a minority carrier lifetime, is not constant but change with time. It is known that a radiative lifetime (τ_{rad}) in $MAPbI_3$ strongly depends on Δn, and τ_{rad} is ~10 ns ($\Delta n \sim 10^{18}$ /cm^3), ~100 ns ($\Delta n \sim 10^{17}$ /cm^3), and ~1 μs ($\Delta n \sim 10^{16}$ /cm^3).[35] Δn can be roughly estimated to be on the order of 10^{18} /cm^3 immediately after the pulse laser irradiation, as mentioned above, and reflected microwave intensity may be proportional to Δn. Based on this consideration, Δn at each

time is roughly estimated, which is added to Fig. 1 together with lifetime values estimated from the slopes of the decay curve. The Δn-dependent lifetime values are similar to the τ_{rad} values in Ref. 35, and the carrier recombination in the as-prepared $MAPbI_3$ film may be basically limited by radiative recombination.

Figure 2 shows decay curves obtained by differential μ-PCD from as-prepared bare and laminated $MAPbI_3$ films. The laminated $MAPbI_3$ film also shows a decay curve with a shape similar to that of the bare film. This indicates that the differential μ-PCD measurement of perovskite films can be performed through module materials such as cover glass and encapsulant used for crystalline Si PV modules. The intensity of the reflected microwave from the laminated film is smaller than that from the bare film. This is partly because of the optical loss of laser pulse light due to reflection and absorption in the glass/encapsulant stack. We separately estimated the optical loss originating from the module materials to be ~20%. Another possible reason for the lower signal intensity in the laminated film is the attenuation of microwave in the glass/encapsulant stack and/or slight thermal degradation of the $MAPbI_3$ film through the lamination process at 110 °C.[24–26)]

Figure 3 shows the decay curves obtained by differential μ-PCD from bare and laminated $MAPbI_3$ films for various air exposure durations. The reduction in the microwave reflection intensity becomes more rapid after longer air exposure, and the rapid decays cannot be explained by the radiative recombination. This clearly indicates the emergence of Shockley-Read-Hall (SRH) recombination and the degradation of $MAPbI_3$ films by air exposure.[35)] It is demonstrated that the degradation of perovskite films can be evaluated by differential μ-PCD. Note that the laminated film shows slower degradation than the bare film, which is given by a protection effect of the lamination

against air exposure. It should also be emphasized that the degradation is also seen in the laminated film. This may be due to the invasion of oxygen and/or moisture from the unsealed edges of the module. Note that no significant changes of the slopes by air exposure are seen near the peak of the decays. One possible explanation for this phenomenon is that radiative recombination is still dominant at a high Δn of 10^{18} /cm^3.[35] Another possible reason is the inaccuracy of the lifetime obtained near the peak of the decay curve since the pulse duration of ~30 ns used in this study is on the same order of the decay.

We finally discuss the advantage of the μ-PCD in the actual industrial application. μ-PCD has been widely utilized for the characterization of Si wafers and can be used in the process line of Si solar cells. Perovskite/Si tandem solar cells and modules will be fabricated in the same process lines as conventional Si cells and modules by adding the processes for perovskite top cells. By switching a pulse laser with a long wavelength of ~900 nm, which is not absorbed in perovskite top cell but absorbed in Si bottom cell, the quality of bottom cells can also be evaluated in the same measurement system. μ-PCD is thus applicable in the production lines of perovskite/Si tandem cells as a quick and non-destructive method to evaluate absorber materials. Another advantage of the usage of μ-PCD is that it can be a portable system and available outdoors.[30] μ-PCD will be utilized for the evaluation of perovskite/Si PV modules in the large-scale PV power plants or other installed sites. This is an advantage of μ-PCD over TRPL, which is also widely used for the carrier lifetime measurement of perovskite films.

In conclusion, we investigated the utilization of differential μ-PCD for the characterization of perovskite films and its time-dependent degradation by air exposure. We demonstrated that differential μ-PCD can measure the carrier lifetime of $MAPbI_3$

films, even after the module lamination with a structure similar to Si solar cells. The decay curve changes with air-exposure duration, and reflected microwave signals drop more rapidly after longer air exposure, which is a clear observation of the degradation of $MAPbI_3$ films. Slower progression of degradation is confirmed in the laminated $MAPbI_3$ films, indicating the protecting effect by the module materials. Differential μ-PCD can be a quick and non-destructive tool for the evaluation of perovskite/Si tandem cells in the cell/module production lines and module-installed sites.

The TPO encapsulant was provided by Dai Nippon Printing Co., Ltd. The authors would like to thank Mr. Shinichiro Hayashi and Ms. Tomoko Hori of Japan Advanced Institute of Science and Technology for their supports for the experiments. This work is supported by the New Energy and Industrial Technology Development Organization (NEDO).

References

1) A. Kojima, K. Teshima, Y. Shirai, and T. Miyasaka, J. Am. Chem. Soc. **131**, 6050 (2009).

2) M. M. Lee, J. Teuscher, T. Miyasaka, T. N. Murakami, and H. J. Snaith, Science **338**, 643 (2012).

3) J. H. Heo, S. H. Im, J. H. Noh, T. N. Mandal, C.-S. Lim, J. A. Chang, Y. H. Lee, H.-j. Kim, A. Sarkar, and M. K. Nazeeruddin, Nat. Photonics **7**, 486 (2013).

4) J.-H. Im, I.-H. Jang, N. Pellet, M. Grätzel, and N.-G. Park, Nat. Nanotechnol. **9**, 927 (2014).

5) D.-Y. Son, J.-W. Lee, Y. J. Choi, I.-H. Jang, S. Lee, P. J. Yoo, H. Shin, N. Ahn, M. Choi, D. Kim, and N-.G Park, Nat. Energy **1**, 16081 (2016).

6) M. Saliba, T. Matsui, K. Domanski, J.-Y. Seo, A. Ummadisingu, S. M. Zakeeruddin, J.-P. Correa-Baena, W. R. Tress, A. Abate, A. Hagfeldt, and M. Grätzel, Science **354**, 206 (2016).

7) N. J. Jeon, H. Na, E. H. Jung, T.-Y. Yang, Y. G. Lee, G. Kim, H.-W. Shin, S. I. Seok, J. Lee, and J. Seo, Nat. Energy **3**, 682 (2018).

8) W. S. Yang, J. H. Noh, N. J. Jeon, Y. C. Kim, S. Ryu, J. Seo, and S. I. Seok, Science **348**, 1234 (2015).

9) M. Ozaki, Y. Nakaike, A. Shimazaki, M. Jung, N. Maruyama, S. Yakumaru, A. I. Rafieh, P. Ekanayake, T. Sato, Y. Shimakawa, T. Sasamori, Y. Murata, R. Murdey, and A. Wakamiya, Bull. Chem. Soc. Jpn. **92**, 1972 (2019).

10) M. Ozaki, Y. Ishikura, M. A. Truong, J. Liu, I. Okada, T. Tanabe, S. Sekimoto, T. Ohtsuki, Y. Murata, R. Murdey, and A. Wakamiya, J. Mater. Chem. A **7**, 16947 (2019).

11) T. Nakamura, T. Handa, R. Murdey, Y. Kanemitsu, and A. Wakamiya, ACS Appl.

Electron. Mater. **2**, 3794 (2020).

12) Y. Cho, J. Bing, H. D. Kim, Y. Li, J. Zheng, S. Tang, M. A. Green, A. Wakamiya, S. Huang, H. Ohkita, and A. W. Y. Ho-Baillie, ACS Appl. Mater. Interf. **13**, 39178 (2021).

13) Md. Shahiduzzaman, S. Fukaya, E. Y. Muslih, L. Wang, M. Nakano, Md. Akhtaruzzaman, M. Karakawa, K. Takahashi, J -M. Nunzi, and T. Taima, Materials **13**, 2207 (2020).

14) Md. Shahiduzzaman, E. Y. Muslih, A. K. M. Hasan, L. Wang, S. Fukaya, M. Nakano, M. Karakawa, K. Takahashi, Md. Akhtaruzzaman, J.-M. Nunzi, T. Taima, Chem. Eng. J. **411**, 128461 (2021).

15) Md. Shahiduzzaman, M. I. Hossain, S. Otani, L. Wang, S. Umezu, T. Kaneko, S. Iwamori, K. Tomita, Y. H. Tsang, Md. Akhtaruzzaman, D. Knipp, J.-M. Nunzi, M. Isomura, J. A. Zapien, and T. Taima, Chem. Eng. J. **426**, 131831 (2021).

16) Md. Shahiduzzaman, D. Kuwahara, M.Nakano, M. Karakawa, K. Takahashi, L. Nunzi, and T. Taima, Nanomaterials **10**, 1676 (2020).

17) Md. Shahiduzzaman, A. Kulkarni, S. Visal, L. L. Wang, M. Nakano, M. Karakawa, K. Takahashi, S. Umezu, A. Masuda, S. Iwamori, M. Isomura, T. Miyasaka, K.Tomita, and T. Taima, Sustain. Energy Fuels **4**, 2009 (2020).

18) J. Werner, B. Niesen, and C. Ballif, Adv. Mater. Interf. **5**, 1700731 (2018).

19) A. Al-Ashouri, E. Köhnen, B. Li, A. Magomedov, H. Hempel, P. Caprioglio, J. A. Márquez, A. B. M. Vilches, E. Kasparavicius, J. A. Smith, N. Phung, D. Menzel, M. Grischek, L. Kegelmann, D. Skroblin, C. Gollwitzer, T. Malinauskas, M. Jošt, G. Matič, B. Rech, R. Schlatmann, M. Topič, L. Korte, A. Abate, B. Stannowski, D. Neher, M. Stolterfoht, T. Unold, V. Getautis, and S. Albrecht, Science **370**, 1300 (2020).

20) M. Jošt, L. Kegelmann, L. Korte, and S. Albrecht, Adv. Energy Mater. **10**, 1904102 (2020).

21) D. Yang, X. Zhang, Y. Hou, K. Wang, T. Ye, J. Yoon, C. Wu, M. Sanghadasa, S. (Frank) Liu, and S. Priya, Nano Energy **84**, 105934 (2021).

22) C. Kamaraki, M. T. Klug, T. Green, L. M. Perez, and C. Case, Appl. Phys. Lett. **119**, 070501 (2021).

23) S. Kim, T. T. Trinh, J. Park, D. P. Pham, S. Lee, H. B. Do, N. N. Dang, V.-A. Dao, J. Kim, and J. Yi, Sci. Rep. **11**, 15524 (2021).

24) N.-K. Kim, Y. H. Min, S. Noh, E. Cho, G. Jeong, M. Joo, S.-W. Ahn, J. S. Lee, S. Kim, K. Ihm, H. Ahn, Y. Kang, H.-S. Lee, and D. Kim, Sci. Rep. **7**, 4645 (2017).

25) T. T. Ava, A. A. Mamun, S. Marsillac, and G. Namkoong, Appl. Sci. **9**, 188 (2019).

26) A. Kumar, U. Bansode, S. Ogale, and A. Rahman, Nanotechnology **31**, 365403 (2020).

27) T. Tiedje, J. I. Haberman, R. W. Francis, and A. K. Ghosh, Appl. Phys. Lett. **54**, 2499 (1983).

28) H. Hashizume, F. Ojima, K. Iba, N. Yoshida, H. Takamatsu, and S. Sumie, IEICE Technical Report **97**, 29 (1997). (in Japanese)

29) K. Ohdaira, H. Takemoto, K. Shiba, and H. Matsumura, Appl. Phys. Express **2**, 061201 (2009).

30) M. A. Islam, D. C. Nguyen, and Y. Ishikawa, Jpn. J. Appl. Phys. **58**, 106507 (2019).

31) N. Nishikawa, S. Yamaguchi, and K. Ohdaira, Microelectron. Reliab. **79**, 91 (2017).

32) T. J. Savenije, A. J. Ferguson, N. Kopidakis, and G. Rumbles, J. Phys. Chem. C **117**, 24085 (2013).

33) T. J. Savenije, D. Guo, V. M. Caselli, and E. M. Hutter, Adv. Energy Mater. **2020**, 1903788 (2020).

34) P. Ščajev, S. Miasojedovas, and S. Juršėnas, J. Mater. Chem. C **8**, 10290 (2020).

35) F. Staub, U. Rau, and T. Kirchartz, ACS Omega **3**, 8009 (2018).

Figure Captions

Fig. 1 Decay curve obtained by differential μ-PCD from an as-prepared bare $MAPbI_3$ film. The inset shows the magnified view of the decay curve near the peak.

Fig. 2 Decay curves obtained by differential μ-PCD from as-prepared bare and laminated $MAPbI_3$ films.

Fig. 3 Decay curves obtained by differential μ-PCD from (a) bare and (b) laminated $MAPbI_3$ films for various air exposure durations.

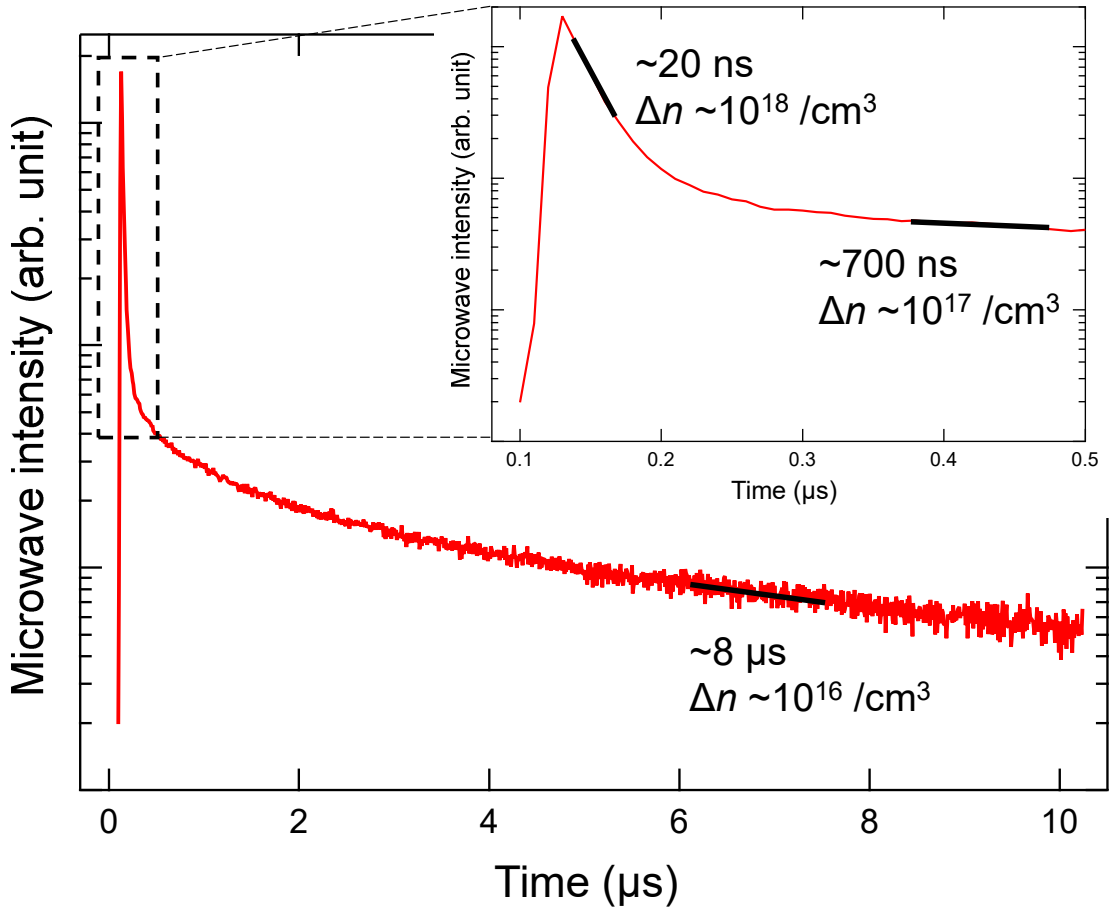

Fig. 1 K. Ohdaira et al.,

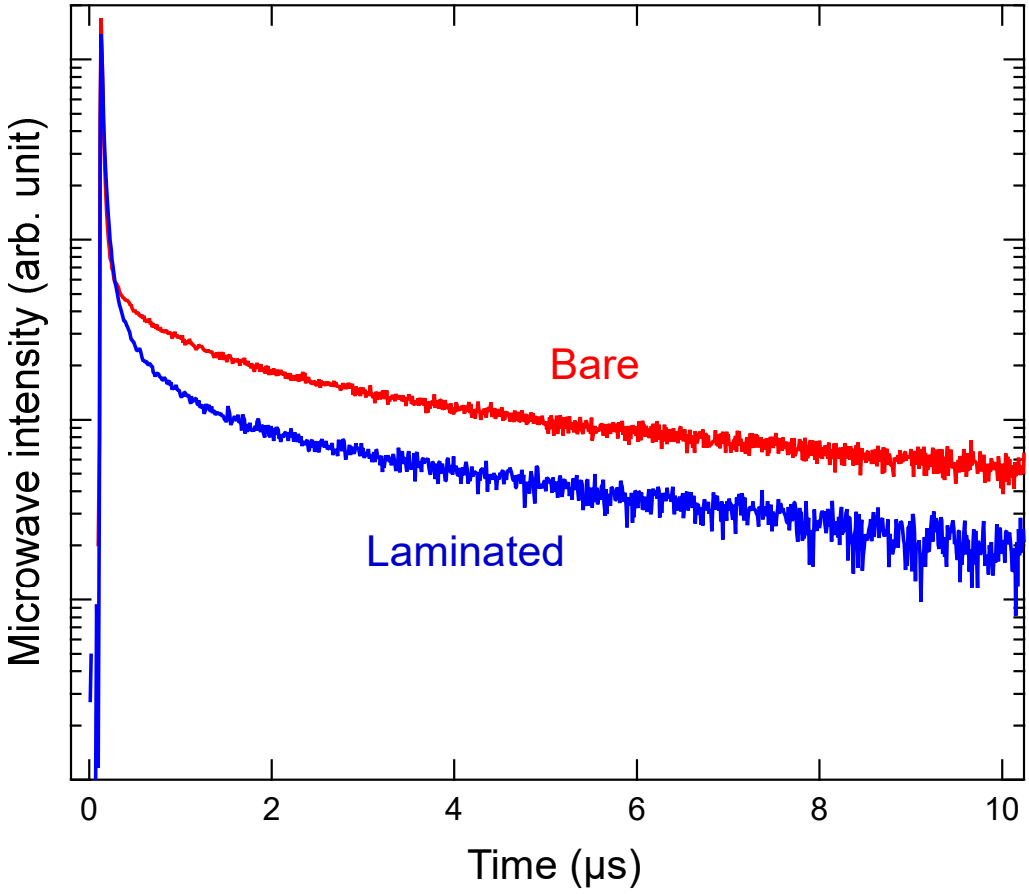

Fig. 2 K. Ohdaira et al.,

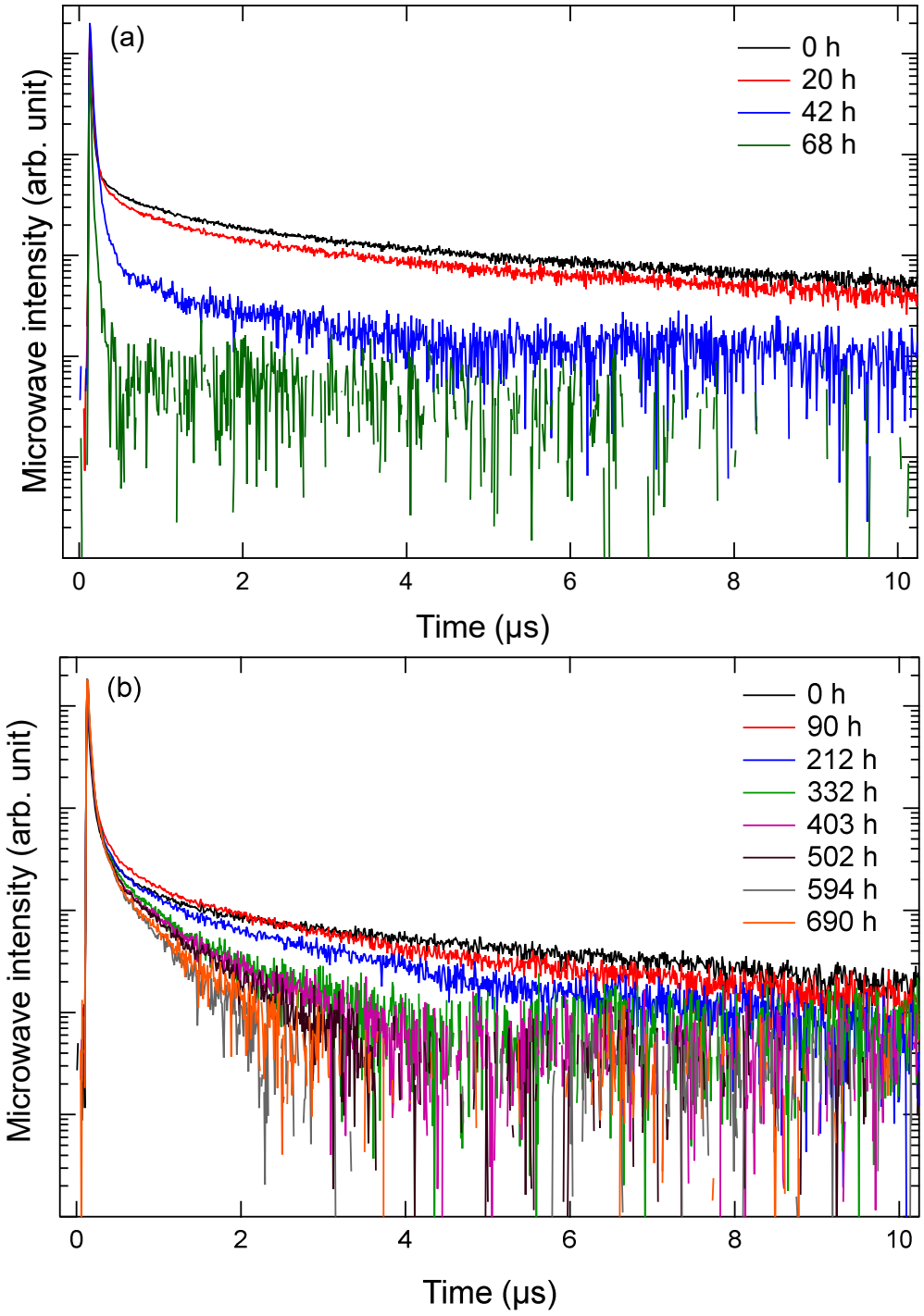

Fig. 3 K. Ohdaira et al.,